Journal of Thermal Analysis and Calorimetry (2023) 148:1981–1995
https://doi.org/10.1007/s10973-022-11868-6

Magnetic cork particles as reinforcement in an epoxy resin: effect of size and amount on thermal properties

J. Abenojar[1,2] · S. Lopez de Armentia[3] · A. Q. Barbosa[4] · M. A. Martinez[1] · J. C. del Real[3] · L. F. M. da Silva[5] · F. Velasco[1]

Received: 20 March 2022 / Accepted: 2 December 2022 / Published online: 28 December 2022

Abstract

Natural brightness of epoxy adhesives can be reduced by adding cork. Besides, when cork was magnetized, it was possible to move them depending on the properties required in each section of the adhesive bond (PAT354/2019). The main objective of this work was to study possible changes in the thermal properties of the adhesive due to the addition of magnetic cork particles. If changes were significant, the use of magnetic cork particles would be compromised. To this end, natural cork particles and magnetic cork particles, with two different particle size (53–38 and 250–125 μm) and percentage (1 and 5 v/v%), were compared as reinforcement material. Magnetic cork was obtained by co-precipitated coating, according to patent number WO2019025651. The thermal properties studied by Differential Scanning Calorimetry were activation energy of curing reaction, glass transition temperature (T_g) and thermal conductivity. Two different hardeners were studied and a factorial design (2^k with $k=4$) was carried out. It allowed to determine which variable or combination of variables had most impact on thermal properties. Results showed that the main parameter affecting thermal properties was the hardener, regardless of the kind of particle used. However, the presence of magnetic cork highlights further the differences found between hardeners. The conclusion of this study was that magnetic cork particles can be used as fillers in epoxy resin to make graded joints, since they do not affect the thermal properties of the resin.

✉ J. Abenojar
abenojar@ing.uc3m.es

1 Materials Science and Engineering and Chemical Engineering Department, In-Service Material Performance Group, "Álvaro Alonso Barba" Institute of Chemistry and Materials Technology, Universidad Carlos III de Madrid, Av. Universidad 30, 28911 Leganés, Spain

2 Mechanical Engineering Department, Universidad Pontificia Comillas, Alberto Aguilera 25, 28015 Madrid, Spain

3 Mechanical Engineering Department, Institute for Research in Technology, Universidad Pontificia Comillas, Alberto Aguilera 25, 28015 Madrid, Spain

4 Instituto de Ciência e Inovacão em Engenharia Mecânica e Engenharia Industrial, Rua Dr. Roberto Frias 400, 4200-465 Porto, Portugal

5 Deparment of Mechanical Engineering, Faculty of Engineering, University of Porto, Rua Dr, Roberto Frias, 4200-465 Porto, Portugal

Graphical abstract

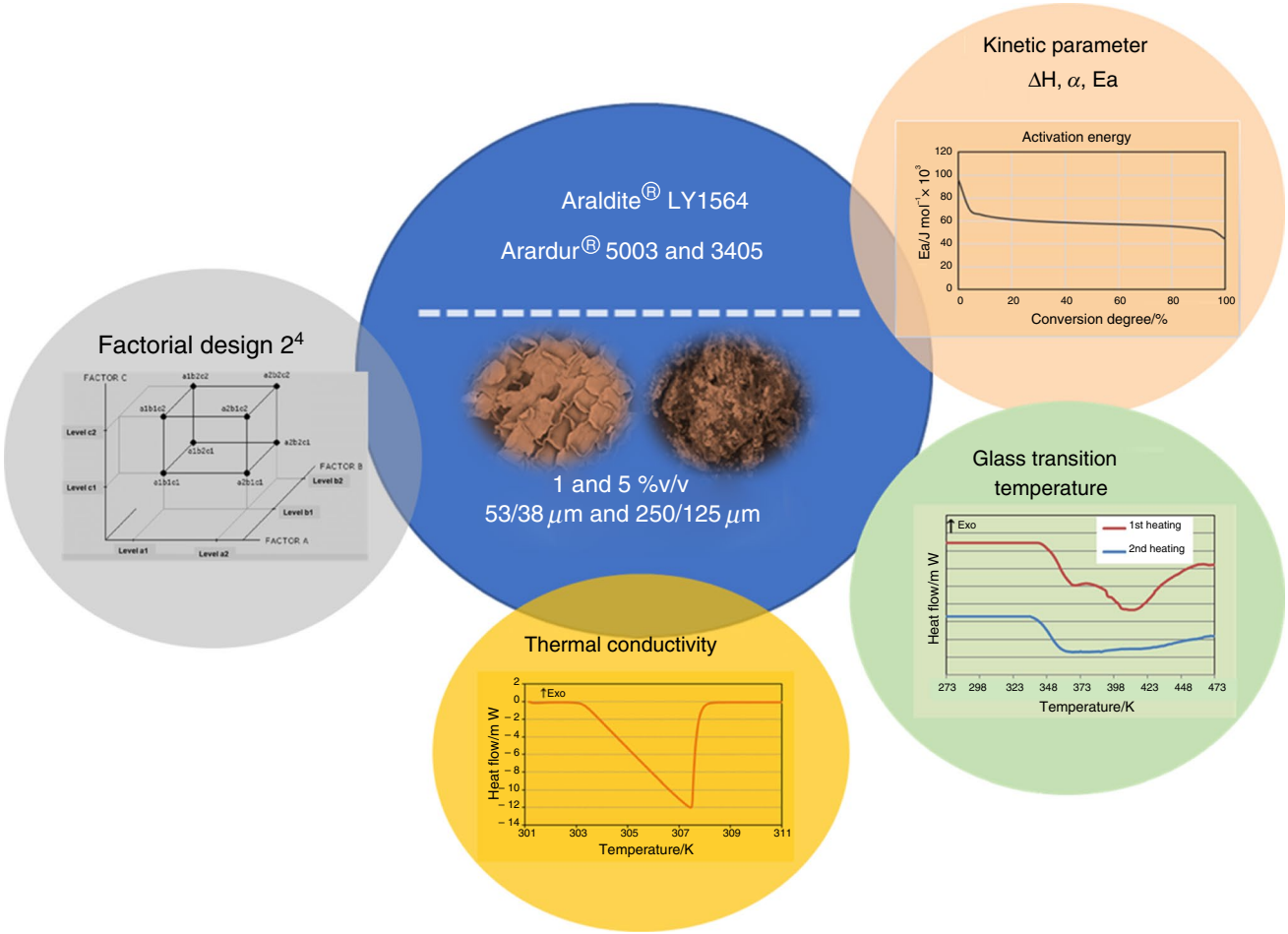

Keywords Polymer composite · Thermal properties · Adhesive · Cork · Magnetic cork

Introduction

To understand the objective of this work, some topics need to be introduced: (i) the current brittleness of epoxy adhesives, (ii) the addition of particulate fillers to these adhesives, (iii) the advantages of graded joints, and (iv) the obtention of magnetic cork to produce graded joints.

Epoxy resins are, along with polyurethanes, the most used structural adhesives in an industrial level. They are synthesized by the reaction of bisphenol A and epichlorohydrin in the presence of sodium hydroxide (NaOH). Once the prepolymers are obtained, an amine (hardener) is added to produce the crosslinking of the resin (Fig. 1). This reaction can be followed through the electron pair of the nitrogen [1].

Epoxy resins are structural adhesives which has good chemical resistance and good mechanical properties, but they are brittle. There are many approaches which try to decrease brittleness to get a more ductile adhesive through the incorporation of reinforcements, such as SiO_2 [2], flexible polymers [3] or nano-clays [4]. Cork can be used to modify the mechanical properties of brittle epoxy adhesives, for example Barbosa et al. [5–7] studied the effect of size, amount, and surface treatment on mechanical properties of epoxy resin reinforcement with cork particles. The addition of cork can give more resistance to the impact, reducing rigidity and increasing tenacity of the adhesive. However, reinforcements modify the whole adhesive, and they may even decrease the resistance.

As a consequence of this brittleness, stress concentrations may find at the end of the overlap for the single lap joint (SLJ). These stress concentrations, although smaller than those that exist in other joining methods, are still significant and can cause problems when joining materials with low through-the-thickness strength [8]. In order to reduce these concentrations and to avoid the decrease in the strength of the adhesive bond, graded joints emerge. These graded

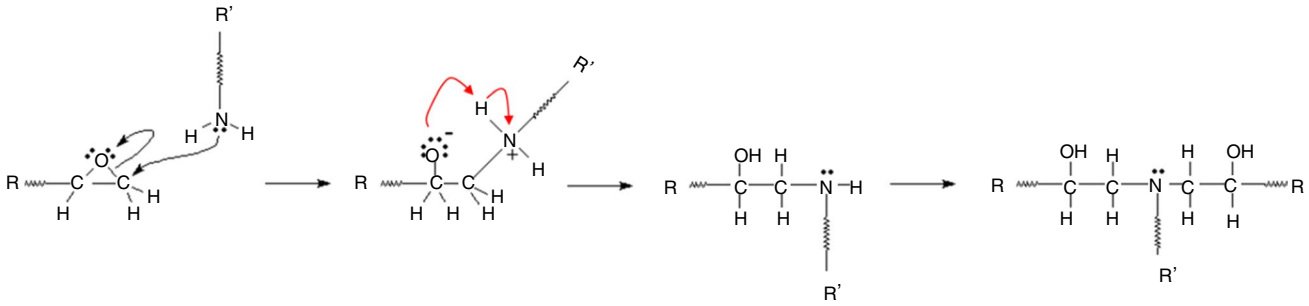

Fig. 1 Scheme of the epoxy resin crosslinking

adhesive joints need to have different properties along adhesive bond. There are several techniques that can be used to improve the joint strength [9], but the focus in this research is only on adhesive-related techniques.

(A) To manufacture adhesive bonding systems of variable stiffness along the bond line, Chiminelli et al. [10] explored this technique for an SLJ and they considered the property variation in discrete steps along the joint length. Galvez et al. [11] used two adhesives with different Young's modulus to make graded adhesive joins. Besides, a simple but effective dry adhesive material for mounting and transporting objects by automated robotic devices was developed using graded adhesion joints [12]. This technique was applied to epoxy resin [11] and acrylic adhesives [13], fundamentally.

(B) The adhesive bond can be cured gradually, so the adhesive will have different T_g in each of the parts, being tougher (lower T_g) at the ends and more rigid (higher T_g) in the center. Carbas et al. [14] changed the adhesive stiffness along the overlap by induction heating, being maximum in the middle and minimum at the ends of the overlap.

(C) Finally, modifying an adhesive with particles, such as rubber [15] or glass beads [16], placed at the edges of the joint can change the stiffness of the adhesive throughout the overlap. The doped adhesive has different densities and can be considered as a functionally graded material. A good method to place particles would be that they can be moved into the resin before curing. If particles have magnetic properties, its concentration can be tailored in each adhesive section by applying a magnetic field. A polyurethane adhesive was loaded with magnetite to improve its properties, the result depended on the amount and distribution of the iron particles [17].

Previous works have proved that cork can be used as reinforcement of adhesives thanks to its density similar to adhesives. Besides, it is possible to manufacture graded joints using magnetic cork. To obtain magnetic cork, first it was treated in a chamber of low-pressure plasma (LPP). LPP increases cork wettability [18] for a better adsorption of the magnetic particles on its surface. Then, the magnetization of the cork was carried out by co-precipitated coating and wet method [19], and it is under Patent Number WO2019025651. The feasibility of the graded adhesive joint with magnetic cork was studied and a methodology and apparatus to manufacture functionally graded joints using magnetized micro particles [20] was developed. It is under Patent number PAT354/2019. On the other hand, magnetic cork/epoxy composite also can be used as a coating on metals since magnetite is a well crystallized form of the iron oxide [21–24]. All these fillers or nanofillers change properties of epoxy resin, like thermal conductivity, electrical conductivity, mechanical and tribological properties [25–28].

There are many scientific papers regarding the effect of particles on thermal properties of composite materials or adhesives. It is well known that the curing reaction of epoxy resin has two mechanisms, auto-catalytic and n-order. The mission of the hardener is to open the oxirane ring that provides OH groups (Fig. 1). These OH groups act as catalysts of reaction and increase the initial reaction rate [29, 30]. The particles can modify the reaction kinetics, accelerating or inhibiting the process. For example, Zeolite particles acted as catalyst for epoxy systems [31], nano-scale aluminum hypophosphite increased T_g and decreased activation energy of curing reaction [32], nano-silica [2] promoted the initial curing mechanism (autocatalytic reaction), but in high amount they hinder crosslinking, and the total curing was inhibited. Among them, the study carried out on the influence of cork particles on the curing of an epoxy resin [33] showed that at lower temperatures of 298 and 323 K, a catalytic effect is observed when the cork particles are added in low percentage (1%). However, 5% cork particles produce a steric hindrance.

From an industrial point of view, the nature and properties of cork make it a very attractive biomaterial widely used in different industries [34–36]. All these industries are continually manufacturing and generating cork waste, which

can be reused and recycled as filler material in composites and adhesives industry.

This work aims to study the effect of magnetic cork on the curing and the thermal properties of an epoxy resin, which is used with two different catalysts. The results will provide information on whether these magnetic particles can be used without a decrease in the thermal properties of the epoxy resin. On the other hand, from an industrial point of view, it is vital to know the curing process, which will define important adhesive parameters as pot life, gel time, and open time. For this, differential scanning calorimetry (DSC) is performed both to calculate the curing kinetics, as well as for the glass transition temperature (T_g) and the thermal conductivity (λ). Furthermore, cork was used in two different proportions (1 and 5 v/v%) and two particle sizes (53–38 and 250–125 μm). These parameters provide 18 different combinations, so a factorial design is made to calculate the parameter or parameters that most influence the properties. According to literature, there is not any research paper regarding thermal properties of epoxy resin filled with magnetic cork particles and it opens the door to new research using these improved adhesives.

Experimental

Materials

The epoxy resin was Araldite® LY 1564, with two different hardeners Arardur® 3405 and 5003 by Huntsman Advanced Materials (Everberg, Belgium). Chemical composition of epoxy resin is 2,2'-[(1-methylethylidene) bis (4,1-phenylenoxymethylien)] bisoxirane (> 70–< 90% w/w) and 1,4-Bis(2,3-epoxypropoxy)butane) (> 10–< 20% w/w), it is clear liquid, whose viscosity is between 0.2 and 1.4 Pa s, and density between 1.10 and 1.20 g cm^{-3} at 298.15 K. The hardener 3405 is essentially amines, α-(2-aminomethylethyl)-Ω-(2-aminomethylethoxy), diethylentriamine and 2,4,6-tris(dimethylaminomethyl)phenol, but it also contains poly[oxy(methyl-1,2-ethanediyl)] and bisphenol A. Resin:hardener ratio is 100:36 mass%. It is a red liquid, whose viscosity is between 70 and 90 mPa s and density between 0.95 and 1 g cm^{-3} at 298 K. Hardener 5003 is only composed for 3,6,9,12-Tetraazatetradecamethylenediamine, it is a clear light-yellow liquid with a viscosity between 0.07 and 0.1 Pa s, density between 0.98 and 1.08 g cm^{-3} at 298 K, and the recommended epoxy:hardener ratio is 100:20 mass%.

Cork particles were supplied by Amorim Cork Composites (Mozelos, Portugal), with two particle sizes: 250–125 and 53–38 μm. To obtain magnetic cork, it was treated in low pressure plasma by Harrick Plasma Cleaner chamber (Ithaca, NY, USA) using air as the gas to produce plasma at a pressure of 40 Pa, for 300 s at 9 W [18]. Then, 2 mass% of cork was introduced into an aqueous acid solution whose molar ionic ratio Fe^{3+}/Fe^{2+} was 2/1. On this solution a basic ammonium solution 2 M was added at 1 drop/s. The final solution was filtered, and cork particles, with adsorbed magnetite on surface, were washed with deionized water until pH 7 and freeze-dried 12 h using a Telstar LyoQuest freeze dryer (Telstar, The Netherlands) [19].

Composite specimens with different amount of cork particles (1 and 5 v/v%) were manufactured. The cork was initially mixed with the resin using a centrifuge mixing machine, Speed-Mixer DAC 150TM by Hauschild Engineering (Hamm, Germany), for 90 s at 1500 rpm, then hardener was added to the mixture. The composites with magnetic cork were compared with neat resin and composite with natural cork. The nomenclature followed for composites is Resin + Hardener + % cork (C) or MC (magnetic cork) particle size, e.g. 1564 + 3405 + 1C_53/38 is 1564 resin and 36 mass% of hardener 3405 to which 1 v/v% cork with a particle size of 53–38 μm has been added.

Characterization of epoxy resin by infrared spectroscopy

Fourier transform infrared spectroscopy (FTIR) was used in this study to determine the functional groups of the resins and the two hardeners. Monitoring of the curing reaction can also be done by FTIR; however, in this case, spectra were performed before curing and after 10 days of curing.

Tensor 27 Fourier-Transform Infrared (FTIR) spectrometer (Bruker Optik GmBH, Madrid, Spain) was used to obtain infrared spectra. Golden Gate attenuated total multiple reflection (ATR) device was attached. Forty two scans were taken and averaged with a resolution of 4 cm^{-1} from 600 to 4000 cm^{-1}.

Curing kinetics of epoxy resin and its composites

Reaction kinetics provides valuable information on the energy required to carry out the curing reaction and the mechanisms involved. The effect of the additions of both types of cork may modify the kinetic parameters. This modification may change the thermal properties of the resin, so it is not recommended.

Activation energy of the curing process was studied by means of non-isothermal DSC scans. Tests were performed from 273.15 to 473.15 K at four different heating rates (β): 5, 10, 15 and 20 K min^{-1}. They were carried out with DSC 882e Mettler Toledo GmbH (Greifensee, Switzerland). One gram of mixture is made to use about 9 mg to make each test. Samples were placed in an aluminum crucible of 40 μL

with a 50 µm hole in the lid. Nitrogen delivered at a rate of 80 mL min^{-1} was used as purge gas.

Although there are a lot of empiric method to calculated activation energy of the curing process, Kissinger method and model-free kinetic (MFK) were used in this work. Kissinger method [37] defines activation energy (E_a) from Eq. (1), where E_a is the curing activation energy (J mol^{-1}), T is the exothermic peak temperature of each curve (K), R is the ideal gas constant (8.314 J mol^{-1} K^{-1}), and C is a constant. The slope of the curve ln (β/T^2) versus the inverse of T corresponds to E_a.

$$\mathrm{Ln}\left(\frac{\beta}{T^2}\right) = -\frac{E_a}{\mathrm{RT}} + C \tag{1}$$

MFK analysis was carried out by using STARe Software (Mettler Toledo, Greifensee, Switzerland). It is an empirical and mathematic model, whose equations were described by Vyazovkin and Wight [38]. This analysis has the following steps: (1) Calculation of conversion degrees (α) from non-isothermal curves, (2) calculation of E_a as a function of α, and (3) simulation of isothermal curves at different temperatures from activation energy results, what is an alternative to iso-conversional methods [39].

Glass transition temperature

T_G (glass transition temperature) is essential to know the working temperature of an adhesive, which can be modified by the addition of fillers. Since it is the working temperature, it is not recommended to drop it. T_g was determined by a sample portion of polymerized resin or composite of about 9 mg. Samples were tested using DSC from 273.15 to 473.15 K at heating rate of 20 K min^{-1}. Due to the specific thermal behavior of thermosets, the standard temperature program employed for polymers consists of two heatings. 1st heating reflects the entire thermomechanical history if the sample. This includes the impact of the production or manufacturing process, storage, as well as sample preparation. After exceeding the glass transition temperature for amorphous polymers, this history is erased. After a controlled cooling, the 2nd heating shows the material properties and is usually used for material characterization. The glass transition occurs over a broad temperature interval and is related to an increase in specific heat. It is not indicated by a peak, but a step of the base line in the endothermal direction. T_g can be overlapped by a relaxation peak, that is due to the elimination of mechanical stress or dissolution of ordered domains (enthalpy relaxation), which is not found in the 2nd heating.

T_g is determined as the midpoint temperature, according to ASTM E1356 standard, midpoint is half of the heat flow difference between the extrapolated onset and the extrapolated end temperature (half-step method).

Three samples were tested for each material after ten days, when the curing process was finished, according to the technical datasheet of the adhesive.

Thermal conductivity

Both epoxy resin and cork are thermal insulators, however magnetic cork can modify thermal conductivity (λ), since it is a metallic oxide. No change in λ of the epoxy resin should occur to maintain the use as an adhesive. To study λ on polymerized samples, the method proposed by Hakvoort et al. [40] and Boddington [41] was used. Conductivity is calculated from Eq. (2), where h is the height of the sample, A is the surface area of the disk samples, S is the slope of the linear side of the melting peak obtained from the heat flow (ϕ) versus temperature curve, which is calculated from $\phi/\Delta T$; where ΔT is temperature gradient. The test error ranges between ± 10% and it is based on the stationary regime, where the heat flow is function of thermal resistance and is proportional to temperature difference.

$$\lambda = \frac{\phi}{\Delta T}\frac{h}{A} \tag{2}$$

Samples were circular disks of polymerized resin or composite with a height of 2 ± 0.1 and 6 ± 0.1 mm in diameter. Gallium was used as calibration reference and it was placed in an aluminium crucible on the sample disk, which was on the DSC sensor. To ensure good heat transfer, oil was applied on both faces of the sample. On the reference sensor, an empty aluminum crucible was placed. With the slopes explained above (S_G and S_S for gallium and sample, respectively), thermal conductivity was calculated using Eq. (3). The reference gallium slope was 16 W m^{-1} K^{-1}.

$$\lambda = \frac{1}{\left(\frac{1}{S_G} - \frac{1}{S_S}\right)}\frac{h}{A} \tag{3}$$

The scan went from 301.15 to 311.15 K at 0.5 K min^{-1}, followed by cooling to—268.15 K at 10 K min^{-1} to ensure the solidification of the gallium after each measurement. Nitrogen was used as purge gas at 50 mL min^{-1} to prevent oxidation of the gallium. At least three measurements of each material were carried out to calculate thermal conductivity.

Factorial design

Factorial experimental design is based on the analysis of different factors that can influence in an experiment. This tool allows to find the best combination of levels given to the factors by checking the appropriate hypothesis related

to the different factors and estimating their effect on the test results and the interaction between factors.

The factorial design was carried out using four variables: hardener, type of cork, particle size and amount added, what provide 16 possible combinations (24). Once the factors were decided and high and low level were set, the test plan was drawn up. Table 1 shows this test plan with all the combinations between factors with the corresponded level for each one. In this case high level (+) corresponds to hardener 5003, magnetic cork, 250–125 µm particle size and 5%v/v of particles. Low levels (−) were considered to be hardener 3405, natural cork, 53–38 µm particle size and 1%v/v.

With the information on this quadratic matrix and the obtained experimental data, it is possible to obtain sixteen data: the average of the response, four effects of main factors, six effects of interaction between two factors and one effect of interaction between five factors. By using Yates' algorithms, influence values were obtained [42–44].

Table 1 Factorial design and test plan

Combinations	Factorial design			
	Hardener/h	Cork/c	Size/s	% v/v
1	−	−	−	−
h	+	−	−	−
c	−	+	−	−
s	−	−	+	−
%	−	−	−	+
h-c	+	+	−	−
h–s	+	−	+	−
h-%	−	−	−	+
c-s	−	+	+	−
c-%	−	+	−	+
s-%	−	−	+	+
h-c-s	+	+	+	−
h-c-%	+	+	−	+
c-s-%	−	+	+	+
h-s-%	+	−	+	+
h-c-s-%	+	+	+	+

Results

FTIR characterization of pristine resins

Figure 2 displays the infrared spectra belonging to 1564 + 3504 and 1564 + 5003 before and after 10 days of curing and peaks are assigned in Table 2. Areas from 600 to 1800 cm^{-1} and from 2600 to 4000 cm^{-1} are quite similar for the two hardeners although some differences related to their composition were found. The characteristic groups of the oxirane in the epoxy resin are located at 1026 (asymmetric stretching vibration C–O–C) and ~910 cm^{-1} (oxirane ring). Besides, another characteristic group appears at 3045 cm^{-1}, which corresponds to the asymmetric C–H vibration of monosubstituted epoxides. Both epoxide peaks (~910 and 3045 cm^{-1}) should disappear after curing, but they are still present in 1564 + 3405 after curing, since 3405 hardener contains bisphenol A. Asymmetric stretching interactions of $–CH_3$ and $–CH_2–$ appear at 2966 and 2916 cm^{-1}, respectively, for 1564 + 3005 and 1564 + 5003. Symmetric vibrations of these groups appear at 2860 cm^{-1}, for $–CH_3$ and at 2820 cm^{-1}, for $–CH_2–$. The asymmetric and symmetric deformation vibration of the

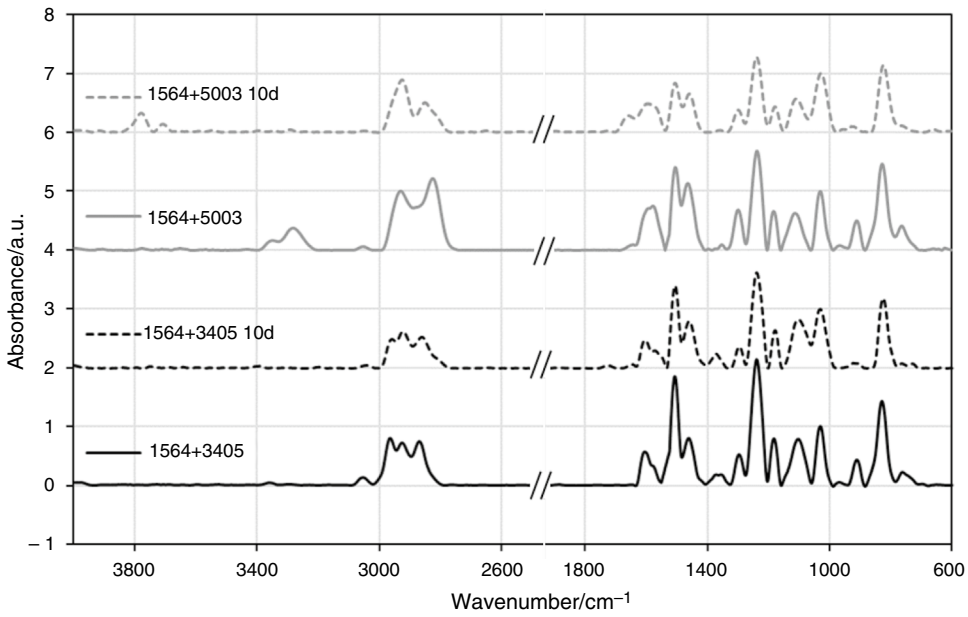

Fig. 2 Infrared spectra for the resin with the two hardeners before and after curing

Table 2 Assignation of bands found in infrared spectra (Fig. 2) for epoxy resin 1564 and hardeners 3405 and 5003 before and after 864,000 s (10 days) curing process

Wavenumber /cm^{-1}	Assignation [45]	H3405	H3405 10d	H5003	H5003 10d
745–760	str R–OH	X		X	
820	str out of plane C–H	X	X	X	X
910–914	Epoxides ring vibration	X		X	
1022–1026	sym str C–O–C	X	X	X	X
1095–1100	asym str C–O–C/str $H_2C–NH_2$	X	X	X	X
1178–1182	str HC–NH_2/in plane C–H	X	X	X	X
1234–1240	str C–O	X	X	X	X
1290	def = C–H in plane	X	X	X	X
1355	sym def OH	X	X		
1450	asym def C–H	X	X	X	X
1502	sym def N–H	X	X	X	X
1568	str N=N/asym def N–H	X	X	X	
1585–1595	str C=C	X	X		X
1620–1640	str C=C aromatic			X	X
2820–2835	sym str-CH_2-			X	X
2855–2865	sym str-CH_3	X	X		
2916	asym str-CH_2-	X	X	X	X
2960–2970	asym str-CH_3	X	X		
3045	asym C–H—epoxides	X	X	X	
3270–3330	str N–H/OH			X	
3690–3750	moisture/OH				X

str stretching; *asym* asymmetric; *sym* symmetric; *def* deformation; epoxides

–CH are at 1452 and 1355 cm^{-1} for 1564 + 3405. However, symmetric vibration is not seen for the resin 1564 + 5003. At 1595 and 1502 cm^{-1}, the stretching bands of the C=C appear for 1564 + 3005. In case of the 1564 + 5003, the band of the C=C were displaced to 1620 and 1508 cm^{-1} what means aromatic groups may be found. Vibration of asymmetric stretching of the oxirane group corresponds to the band at $1290{\cdot}10^{-2}$ m^{-1}, although this band can also correspond to the wagging/bending vibration of the OH group or deformation in the plane of the =C–C groups, to which has been attributed in Table 2 for being the most possible. Vibration of stretching of the C-H link out of the plane and in the plane can also be observed at 827 and 1183 cm^{-1}, respectively, both corresponding to the aromatic ring. Although at 1180 cm^{-1} is also possible to find the stretching vibration of CH–NH_2, whereas the stretching vibration of CH_2–NH_2 appears at 1100 cm^{-1} overlapped with asymmetric stretching vibration of C–O–C. Finally, the band at 760 cm^{-1} is typically due to the diglycidyl ether structure of an epoxy before the complete curing process. There are some cork peaks that overlap with those of the resin, such as those belonging to the OH and C–H and therefore do not serve to identify the cork. Even the peaks found in cork at 1730 cm^{-1} (C=O) and the one corresponding to the C=C bond at 1512 cm^{-1} [19], cannot be clearly observed in the spectra. Therefore, the amount of cork added does not give a signal high enough to discern it from those of the resin.

Kinetics of the curing process

Figure 3 shows the curves at different rates for mixture 1564 + 3405 + 1MC_53/38. Similar plots were found for all mixtures studied. When rate increases, the curing peak moves to higher temperature, height is higher, but width is lower than other curves with lower rates. Therefore, the

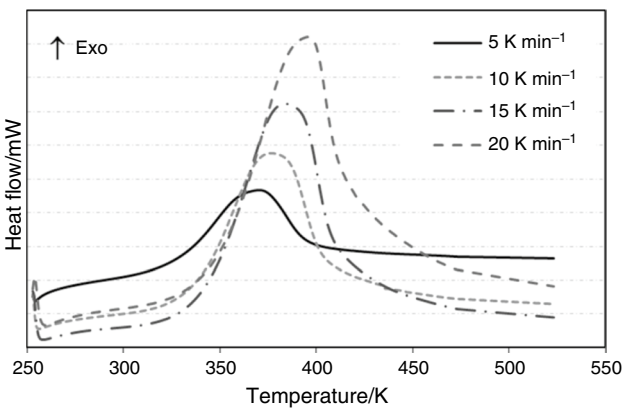

Fig. 3 Curing curves at different rates for 1564 + 3405 + 1MC_53/38

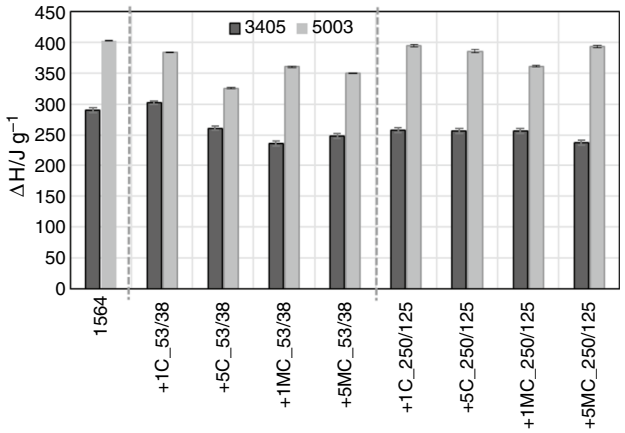

Fig. 4 Enthalpy of curing for all samples

area under the curve keeps constant and its value is the curing enthalpy (ΔH). The integration of the four curves with different rates for each mixture provided ΔH (Fig. 4). The error bars represent the standard deviation between the four curves.

ΔH is higher for mixtures with hardener 5003 (Fig. 4), around 28% higher than mixtures with hardener 3405. When adding both, cork and magnetic cork, ΔH decreases in all cases except for the mixture 1564 + 3405 + 1C_53/38, which increases a 4%. Decrements found vary with the percentage of addition, cork type and size. The biggest drop is 19% for 1564 + 3405 + 1MC_53/38 and 1564 + 5003 + 5C_53/38, followed by 1564 + 3405 + 5MC_250/125 with 18% of decrease. Decreases below 5% are only observed for hardener 5003 in the case of the mixture with + 1C_53/38 (5%), + 1C_250/125 (2%), + 5C_250/125 (4%) and 5MC_250/125 (2%). For the rest of the mixtures the decrements vary from 10 to 15%. The difference in the chemistry of hardeners is responsible for the changes in ΔH. The small decreases can be attributed to the addition of cork, but there is no logical explanation to understand bigger decrements. However, reactions between the cork and the amine of the hardener may be produced by the presence of OH groups in the cork. It seems that the reaction between cork and hardener is easier than with oxirane rings and it release less ΔH. In addition, as the percentage of cork increases, the decrease in ΔH is higher. This agrees with a greater amount of OH groups. However, in the case of magnetic particles the decrease in ΔH when increasing the percentage is lower. This may be due to the fact that magnetic particles having magnetite on the surface have less OH groups on the surface. Other factors that may play a role are density and particle size. The 53/38 µm cork has a density of 1.6 g cm-3 and a D50 of 25 µm, while the magnetic cork has a density of 1.85 g cm-3 and a D50 of 45 µm. Therefore, it seems that in the case of magnetic particles the effect of the OH is not so important, producing a synergistic effect due to the size of the particles and the higher mass. On the other hand, the error due to sample preparation for DSC may also slightly affect the measurements, since for each curve one gram of sample is prepared, using only 9 mg.

For hardener 5003, the largest particles have a different behavior as they tend to agglomerate. Therefore, their specific surface area is smaller and fewer OH groups will be in contact with the adhesive.

When curing curves are partially integrated with respect to time, the conversion degree curves are obtained, according to the Eq. (1) (Fig. 5A). To obtain reliable results, these curves cannot cross, and from them, activation energy of the curing process is calculated applying MFK model, where *Ea* is obtained as a function of the degree of conversion (Fig. 5B).

E_a with respect to the degree of conversion (Fig. 5B) changes as the reaction progress and the reaction mechanism changes. This process can be divided into three stages:

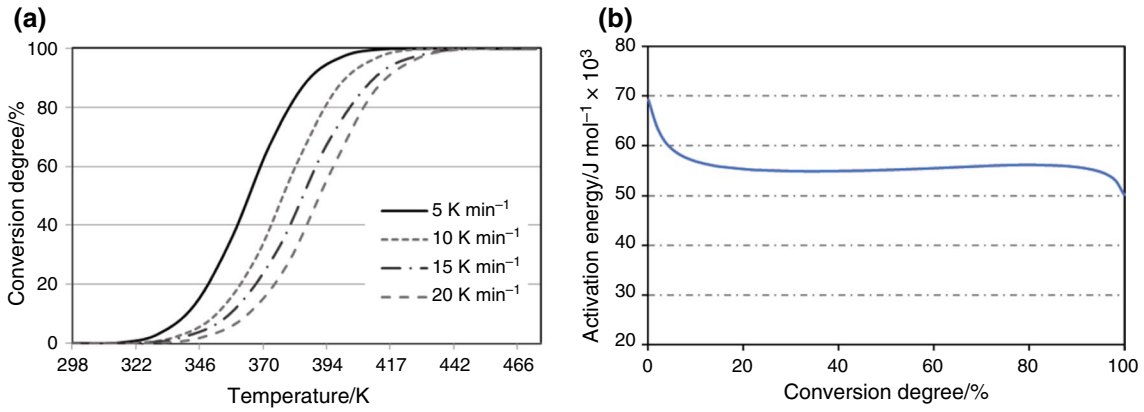

Fig. 5 **A** Curves of conversion degree and **B** Activation energy curve for 1564 + 5003 + 5MC_250/125

i. At the beginning of the reaction, the action of the amine (hardener) with the epoxy resin produces the opening of the oxirane ring and produces OH^-. The initial mechanism is slower and requires more energy to progress, it is a mechanism of *n* order. This process goes approximately up to a degree of conversion of 20 or 25%.

ii. The formation of the OH^- groups accelerate the reaction since they autocatalyze it. They change the initial mechanism from order *n* to autocatalytic. This mechanism occurs from 20–30 to 80–85%, and E_a of the process remains practically constant during this stage. Crosslinking of the resin occurs rapidly.

iii. The last part of the reaction (from 80–85 to 100%) can happen in two different ways, but in this case (Fig. 5B), E_a of the process decreases slightly. According to the literature, the reaction mechanism should change again to order n and be slower with a higher energy input. This is because it is more difficult for the OH and unreacted amines to find each other since the crosslinking of the resin is already high and, therefore, the chains movement is restricted. It can also happen that the ether groups (R–O–R') of lignin or cellulose of the cork react with the amine (cheating the reaction), because of its similarity to epoxy. This would lead to a faster first stage i, but the lack of amine would cause a rather pronounced increase in E_a at the end of the stage iii. However, with these hardeners this is not likely to occur because they contain mixtures of amines, and even hardener 3405 contains bisphenol A.

To compare E_a curves of the two base resins and the mixtures with the different types of cork (eight mixtures per base), the E_a at 5, 50 and 95% of the conversion degree are represented in Fig. 6, where Kissinger E_a is also shown. Thus, Fig. 6A corresponds to hardener 3405 and Fig. 6B to hardener 5003.

In relation to the hardener 3405 (Fig. 6A), all mixtures have initial E_a higher than mixture base. On the other hand, E_a increases for the smallest particle size, for a greater number of particles added, and when the particles are coated. Thus, the highest E_a (practically twice the base) corresponds to the mixture 1564 + 3405 + 5MC_53/38. It could be due to the increase in viscosity that the addition of particles produces, that results in a decrease in reactants mobility.

E_a at 50% conversion is similar for all compounds (Fig. 6A), although slightly lower for mixtures with cork. It could be due to the presence of OH on cork surface that counteract the steric hindrance found in stage i. This energy also coincides with the E_a obtained by the Kissinger equation, around $60{\cdot}10^3$ J mol^{-1}. Besides, at 95% the values are around $40{\cdot}10^3$ J mol^{-1}, although there is gradual

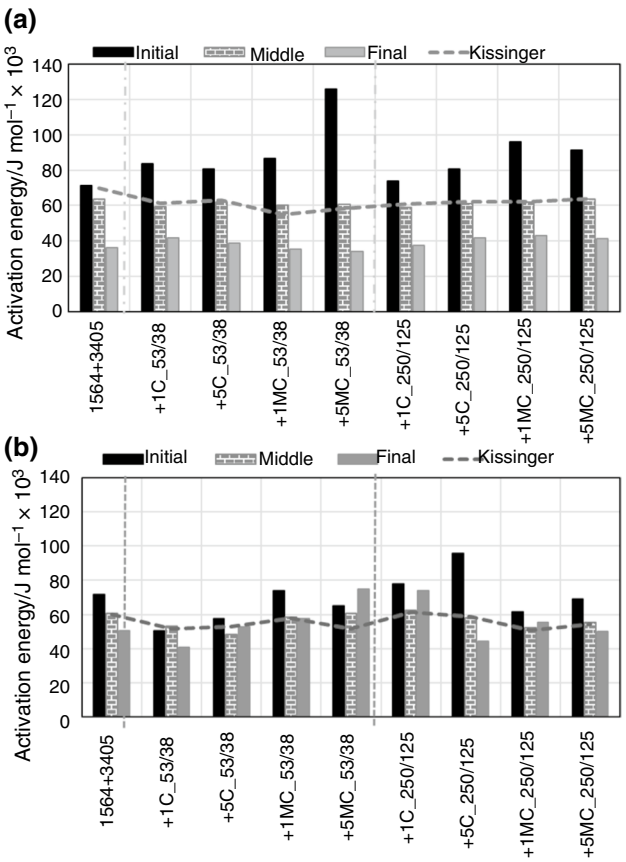

Fig. 6 Activation energy for the three stages of MFK model and Kissinger activation energy. **A** Hardener 3405 and **B** Hardener 5003

increase for particles of 250/125 µm, that is around 20% for 1564 + 3405 + 1MC_250/125 (Fig. 6A).

When the hardener 5003 is used (Fig. 6B), E_a has different tendency, although initial and middle E_a is similar for both hardeners ($72{\cdot}10^3$ and $61{\cdot}10^3$ J mol^{-1} for the hardener 5003 and $71{\cdot}10^3$ and $64{\cdot}10^3$ J mol^{-1} for hardener 3405). With this hardener small particles (53/38 µm) decrease the initial E_a a 30, 20 and 9% for 1 and 5% of cork and 9% for 5% of magnetic cork, but E_a increases a 3% for 1% of magnetic cork. In the case of larger particles (250/125 µm) initial E_a increase around 9 and 33% for 1 and 5% of cork, respectively, whereas E_a decreases for 1 and 5% of magnetic cork a 14 and 4%. The larger the particles, the more initial E_a is needed. This may be due to steric hindrance what do more difficult than amines can open oxirane rings.

E_a at 50% of conversion degree decreases for all the mixtures except for 1564 + 5003 + 1C_250/125 that it increases a 3% (Fig. 6B). The decrements mean that the autocatalytic reaction is faster when there are cork particles than for the neat resin thanks to the OH groups that helps to catalyze the reaction. The lower values of E_a correspond to + 5C_53/38, + 1MC_250/125 and + 1C_53/38, with a decrement of 20, 14 and 13%, respectively. Smaller decreases

Table 3 Simulation of isothermal curing at different temperatures for 1564 + 3405 + 5C_250/125

Conversion degree/%	Time/s × 10^3				
	Temperature/K				
	298	313	333	353	373
10	5.55	1.54	0.33	0.09	0.03
20	8.22	2.43	0.57	0.16	0.05
30	10.96	3.32	0.80	0.23	0.07
40	14.22	4.36	1.06	0.30	0.10
50	18.32	5.64	1.38	0.40	0.13
60	23.46	7.22	1.77	0.51	0.17
70	29.93	9.21	2.26	0.65	0.21
80	32.97	11.75	2.90	0.84	0.28
90	32.98	12.40	3.33	1.08	0.40
95	32.99	12.40	3.40	1.26	0.52

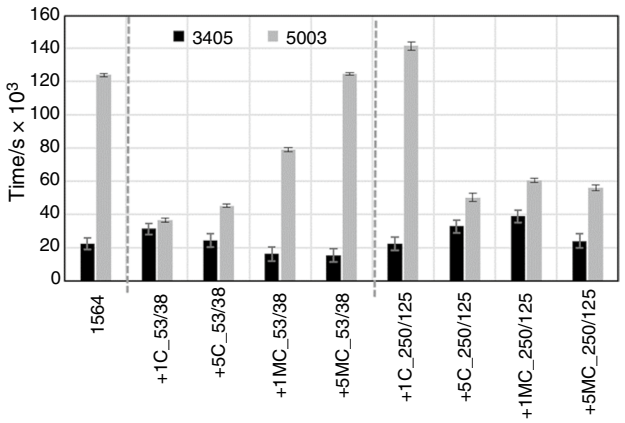

Fig. 7 Curing process simulation at 298.15 K at 95% of conversion degree for both resins and composites

are found for the remaining mixtures. As for hardener 3405, middle E_a is similar to Kissinger E_a.

The third stage of the reaction with hardener 5003 is different from that found with the other hardener (Fig. 6B). For almost all the mixtures the E_a is higher or equal than for the neat resin, except for + 1C_53/38 and + 5C_250/125. For 3405 hardener, final E_a never exceeds middle E_a. However, with the hardener 5003 there are some cases that exceed it, even for the mixture it exceeds the initial one (+ 5MC_53/38).

From the activation energy curves, STARe Software allows simulations of isothermal processes at different temperatures, as shown in Table 3 for composite 1564 + 3405 + 5C_250/125. As expected, when the temperature increases the curing process is faster.

Figure 7 shows the simulation for both resins and their composites. Curing time for resin 1564 + 3405 is lower than for 1564 + 5003, from 22,620 to 156,420 s. Coherently, composites for 3405 also have lower activation energy than composites for 5003. The behavior of the particles is different depending on the hardener. Thus, small particles increase curing time slightly for 1564 + 3405 + 1C in relation to neat resin. However, for + 5C, + 1MC and + 5MC curing time decreases in that order. However, small particles decrease curing time for 1564 + 5003 + 1C and then it gradually increases until 1564 + 5003 + 5MC, where it reaches neat resin. This means that small particles speed up the curing process for both hardeners, but at different rates, e.g. + 5MC does not influence the curing time, but + 1C inhibits slightly the cure of 1564 + 3405, whilst speeds up that of 1564 + 5003.

The behavior of the big particles is different, for the 1564 + 3405 resin the curing time increases (Fig. 7), slightly inhibiting the reaction, while the big particles reduce it to more than half, for the 1564 + 5003. According to Fig. 6B, the higher final activation energy for 1564 + 5003 + 1C_250/125 explains the higher time that is necessary to finish the reaction process. However, a higher initial activation energy is not related to time. This is due to different mechanism, high final activation energy may be due to an inhibition in the curing reaction, while high initial activation energy may be due to an initial acceleration.

Glass transition temperature

The samples used for kinetic study at 20 K min^{-1} were scanned again to calculate the T_g of material. T_gs were 351 ± 2 and 355 ± 2 K, respectively, for epoxy resin 1564 + 3405 and 1564 + 5003.

However, all the samples 1564 + 3405 tested after 864,000 s (10 days) have a curing peak of around 11 J g^{-1}, which represents around 4% of uncured resin. The epoxy resin 1564 + 5003 also has a curing peak of 24 J g^{-1}, when it was tested after 864,000 s (10 days), this is a 6% of total curing enthalpy (Fig. 4). Consequently, for measuring T_gs, a postcuring was carried out. For epoxy resin 1564 + 3405, it was 28,800 s (8 h) at 353.15 K and for 1564 + 5003 it was 7,200 s (2 h) at 353.15 K, according to technical sheet.

This lack of curing shows that the kinetic study was not carried out for 100% of curing. The E_a and simulated isothermal curing times are for 96 and 94% curing, for resin 1564 + 3405 and 1564 + 5003, respectively. Since the empirical methods for determining the kinetic parameters are unreliable for values above 95% curing, the data obtained are in the error range of the method. At the same time, the small percentage of uncured resin is not detected in the infrared spectra.

Figure 8A and Table 4 present T_gs of the epoxy resin 1564 + 5003 and their composites. 1st heating shows a T_g at 378.15 K overlapped with enthalpy relaxation peak ($\Delta H = 2.32$ J g^{-1}), which disappears in the 2nd heating

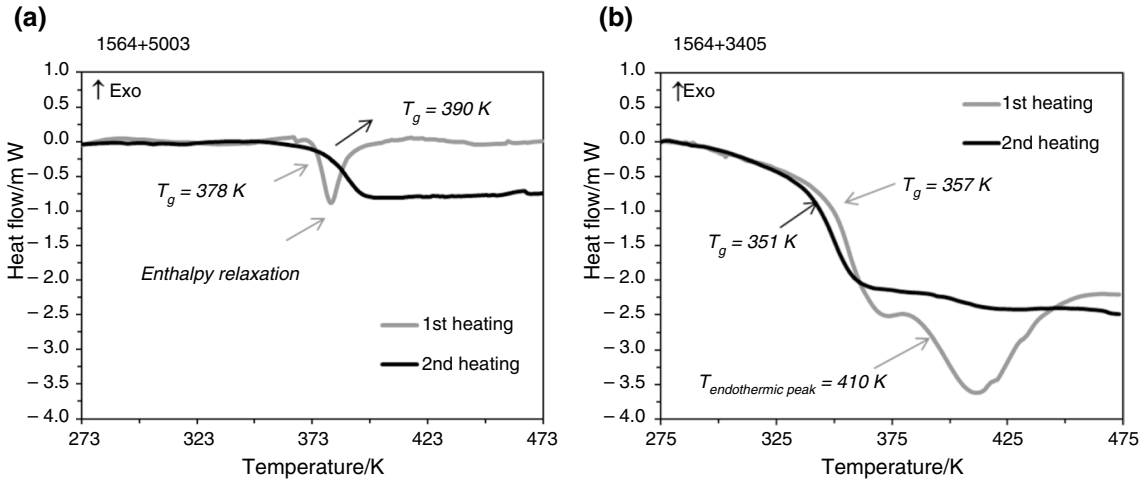

Fig. 8 Dynamic heating to calculate T_g **A** 1564 + 5003 and **B** 16,564 + 3405

Table 4 T_gs of both epoxy resins and their composites for 2nd heating

Material	2nd Heating T_g/K	Material	2nd Heating T_g/K
1564 + 5003	390	1564 + 3405	351
+ 1C 53/38	388	+ 1C 53/38	357
+ 5C 53/38	386	+ 5C 53/38	356
+ 1MC 53/38	387	+ 1MC 53/38	353
+ 5MC 53/38	389	+ 5MC 53/38	353
+ 1C 250/125	389	+ 1C 250/125	351
+ 5C 250/125	383	+ 5C 250/125	353
+ 1MC 250/125	385	+ 1MC 250/125	353
+ 5MC 250/125	386	+ 5MC 250/125	355

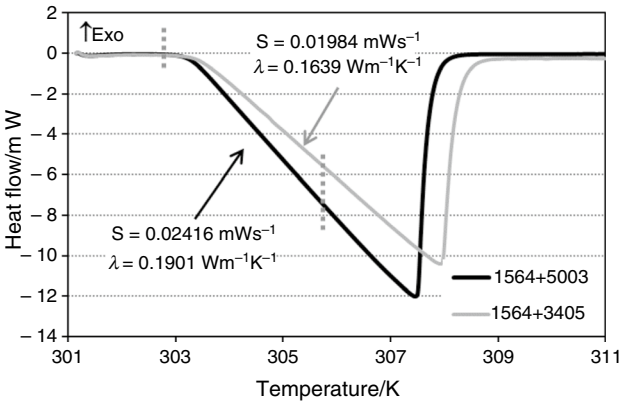

Fig. 9 Dynamic heating to calculate thermal conductivity for both epoxy resins. The slope is measured between the red lines that represent the onset and end temperature

and T_g increases to 390.15 K. This is commonly found for others epoxy resin and it can be seen for all composites of the resin 1564 + 5003 (Fig. 8A). There are not differences between all composites of this resin, with an average value of 387 ± 2 K (Table 4). However, 1564 + 3405 (Fig. 8B) shows a 1st heating a T_g at lower temperature (357 ± 3 K), without enthalpy relaxation peak, T_g is followed by an endothermal peak at approx. 411.15 K and a reaction enthalpy of 8 ± 1 J g^{-1}. This endothermal peak can be due to dissolvent evaporation or decomposition of some component. T_gs in 2nd heating for resin 1564 + 3405 decreases until 351 ± 2 K (Fig. 8B and Table 4), which can be caused by the decomposition of some component, which affected at crosslinking of the resin. When cork or magnetic cork were added to resin 1564 + 3405, T_g in the 2nd heating (average value 353 ± 2 K) decreases slightly in relation to the 1st heating (average value 356 ± 3 K) (Table 4). Besides, for composites the 1st heating enthalpy endothermal peak decreases until $\Delta H = 5 \pm 2$ J g^{-1}. This decrement may be due to a bonds between some cork groups, as ether groups, with some amine of epoxy resin.

With these results, it can be concluded that the crosslinking degree that hardener 5003 provides is higher than 3405. In addition, crosslinking is not overly affected by the presence of the particles, although there is a tendency to decrease T_g for composites in relation to the 1564 + 5003 epoxy resin, being this drop a little higher for larger particles than small ones, in general terms.

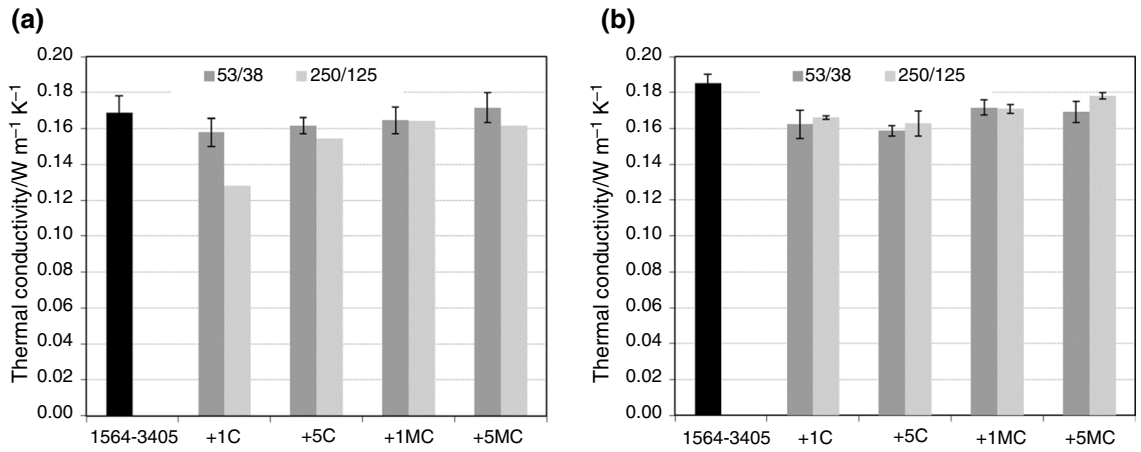

Fig. 10 Thermal conductivity to resin with hardener **A** 3405 and **B** 5003 and their composites

Thermal conductivity

Dynamic heating to calculate λ for both resins are shown in Fig. 9. The difference in the slopes of melting point to the gallium metal provides different λ for them, according to Eq. (3). The slope is measured between the dotted gray lines (Fig. 9) that represent the onset and end temperature.

Figure 10 display λ for all the materials studied. 1564 + 5003 resin has higher λ than 1564 + 3405 resin. This would agree with the shorter chains on the 1564 + 5003 resin and more complex functional groups of the curing agent, while the crosslinking degree affects inappreciably [46].

When cork is added to the 1564 + 3405 resin, λ decreases from 7 to 4% progressively as the percentage of cork raises and continues to raise in the same way with magnetic cork increasing its value by 2% for + 5MC, when the particles are small. The big particles also decrease λ, but to a greater extent than the small ones, especially for the + 1C composite (the drop is 24%), for the + 5C, + 1MC and + 5MC composites λ decreases an 8, 3 and 4%, respectively.

On the other hand, for 1564 + 5003 composites, λ decreases in relation to resin. Conductivity is related to free volume, thus, the higher conductivity the lower free volume [47]. The λ values for composites are similar to those obtained for the other hardener (1564 + 3405), around 0.16 W m^{-1} K^{-1}. In this case, magnetic cork increases a bit more than natural cork and λ for big particles is slightly higher than λ for small particles. However, there is 10% uncertainty in this method to measure λ, consequently, the values are in the uncertainty range of the exploited experimental method for both epoxy resin.

Factorial design

To understand which of the variables have the greatest influence on the studied thermal properties, a 2^4 factorial design is performed.

Hardeners were significantly different, both in curing conditions and in the properties obtained. In addition to obtain all the possible interactions for all the variables studied, a matrix was made. According to Table 1, the matrices have 16 rows and 16 columns and there are as many matrices as properties are studied. Each value of this matrix is calculated according to the Yates' algorithms, the Table 1 and the results of this work. Table 5 shows eight columns for the property λ, the averages of all the columns are compared and the top value is assigned 100 and the rest are recalculated relative to it. From these averages the most significant influences and interactions were obtained.

Therefore, in the case of λ the factor with the greatest influence is the magnetization of cork. Besides, if particle size and hardener were changed at the same time, it would have a high impact on λ. However, the factors with less influence were % and h*c. It means that an increase in particles percentage did not change thermal conductivity in a high extent. In the case of hardener and cork type, their change would lead to a slight decrease in thermal conductivity.

In the case of T_g, ΔH, Kissinger activation energy, initial and final activation energy, similar tables to Table 5 report that the factor with the highest influence was the hardener. However, the sign of the coefficient changed depending on the parameter: it was positive for T_g, ΔH and final activation energy, and negative for Kissinger and initial activation energy. The positive sign means that hardener 5003 showed a higher value than 3405. Therefore, it may be concluded that hardener 5003 resulted in a higher crosslinking density and curing degree, but it is more difficult to finish the curing reaction. In the case of hardener 3405 the reaction

Table 5 Matrix example for thermal conductivity

Combinations	h	c	s	%	h*c	h*s	h*%	c*s
1	−0.158	−0.158	−0.158	−0.158	0.158	0.158	0.158	0.158
h	0.162	−0.162	−0.162	−0.162	−0.162	−0.162	−0.162	0.162
c	−0.165	0.165	−0.165	−0.165	−0.165	0.165	0.165	−0.165
s	−0.128	−0.128	0.128	−0.128	0.128	−0.128	0.128	−0.128
%	−0.162	−0.162	−0.162	0.162	0.162	0.162	−0.162	0.162
h-c	0.172	0.172	−0.172	−0.172	0.172	−0.172	−0.172	−0.172
h–s	0.166	−0.166	0.166	−0.166	−0.166	0.166	−0.166	−0.166
h-%	0.159	−0.159	−0.159	0.159	−0.159	−0.159	0.159	0.159
c-s	−0.164	0.164	0.164	−0.164	−0.164	−0.164	0.164	0.164
c-%	−0.172	0.172	−0.172	0.172	−0.172	0.172	−0.172	−0.172
s-%	−0.155	−0.155	0.155	0.155	0.155	−0.155	−0.155	−0.155
h-c-s	0.171	0.171	0.171	−0.171	0.171	0.171	−0.171	0.171
h-c-%	0.169	0.169	−0.169	0.169	0.169	−0.169	0.169	−0.169
c-s-%	−0.162	0.162	0.162	0.162	−0.162	−0.162	−0.162	0.162
h-s-%	0.163	−0.163	0.163	0.163	−0.163	0.163	0.163	−0.163
h-c-s-%	0.178	0.178	0.178	0.178	0.178	0.178	0.178	0.178
Average	0.00925	0.0125	−0.004	0.00425	−0.0025	0.008	−0.00475	0.00325
	74	100	−32	20	−20	64	−38	26

may be occurred more easily, but the obtained polymer was less crosslinked. However, it is important to keep in mind that both resins need to be cured at 356 K to complete the curing reaction. In the case of the 3405 hardener, temperature needed to be applied for 8 h and for 2 h for the 5003 hardener.

Conclusions

The main parameter that affects both curing process and thermal properties is the chemical composition of the hardener, i.e., with or without phenol. Curing enthalpy, T_g and λ are lower for 3405 (amines + phenol) than 5003 (amines) hardener. Another important difference is simulation curing time at 25% of conversion: 1564 + 3405 epoxy resin only needs around 24,000 s to cure while 164 + 5003 needs around 126,000 s. It can also be seen in the values of activation energy for the different curing stages. It is important to highlight that both hardeners need a post-curing process to achieve 100% of curing degree, being the post-curing times different for both compositions: 5003 needs less time to achieve the complete curing than 3405.

The addition of both cork and magnetic cork does not produce significant differences in the curing process or the thermal properties of epoxy resin, regardless of the hardener used. The effect of the kind of hardener and the addition of cork and magnetic cork particles has been analyzed by factorial design.

Therefore, the main conclusion that can be drawn from this study is that it is feasible to reinforce epoxy resin with magnetic cork to produce graded adhesive joints without changing curing and application parameters.

Author contributions JA: term, conceptualization, methodology, validation, formal analysis, investigation, data curation, writing—original draft, writing—review and editing, visualization, project administration. SLA: investigation, data curation, writing—original draft, writing—review and editing. AQB: resources, writing—original draft. MAM: formal analysis, investigation, data curation, supervision, funding acquisition. JCdR: resources, writing—review and editing, supervision, funding acquisition. LFMdS: resources, writing—review and editing, funding acquisition. FV: resources, writing—review and editing, funding acquisition.

Funding Funding for APC: Universidad Carlos III de Madrid. Open Access funding provided thanks to the CRUE-CSIC agreement with Springer Nature.

References

1. Ouellette RJ, Rawn JD. Alcohols: reactions and synthesis. In: Organic chemistry: structure, mechanism. London: Elsevier; 2019. p. 463–505.
2. Abenojar J, Tutor J, Ballesteros Y, del Real JC, Martínez MA. Erosion-wear, mechanical and thermal properties of silica filled epoxy nanocomposites. Compos B Eng. 2017. https://doi.org/10.1016/j.compositesb.2017.03.047.
3. Li J, Wang H, Li S. A novel phosphorus-silicon containing epoxy resin with enhanced thermal stability, flame retardancy and mechanical properties. Polym Degrad Stab. 2019. https://doi.org/10.1016/j.polymdegradstab.2019.03.020.
4. Withers GJ, Yu Y, Khabashesku VN, Cercone L, Hadjiev VG, Souza JM, Davis DC. Improved mechanical properties of an epoxy glass–fiber composite reinforced with surface organomodified nanoclays. Compos B Eng. 2015. https://doi.org/10.1016/j.compositesb.2014.12.008.
5. Barbosa AQ, da Silva LFM, Abenojar J, Figueiredo M. Analysis of the effect of size, amount and surface treatment on the tensile strain of a brittle adhesive reinforced with micro cork particles. Appl Adhes Sci. 2017. https://doi.org/10.1186/s40563-017-0088-6Online.
6. Barbosa AQ, da Silva LFM, Carbas RC, Abenojar J, del Real JC. Influence of the size and amount of cork particles on the toughness of a structural adhesive. J Adhes. 2012. https://doi.org/10.1080/00218464.2012.660811.
7. Barbosa AQ, da Silva LFM, Abenojar J, Figueiredo M, Ochsner A. Toughness of a brittle epoxy resin reinforced with micro cork particles: effect of size, amount and surface treatment. Compos B Eng. 2017. https://doi.org/10.1016/j.compositesb.2016.10.072.
8. Carbas RJC, da Silva LFM, Andrés LFS. Functionally graded adhesive joints by graded mixing of nanoparticles. Int J Adhes Adhes. 2017. https://doi.org/10.1016/j.ijadhadh.2017.02.004.
9. dos Reis MQ, Marques EAS, Carbas RJC, da Silva LFM. Functionally graded adherends in adhesive joints: an overview. J Adv Join Process. 2020. https://doi.org/10.1016/j.jajp.2020.100033.
10. Chiminelli A, Breto R, Izquierdo S, Bergamasco L, Duvivier E, Lizaranzu M. Analysis of mixed adhesive joints considering the compaction process. Int J Adhes Adhes. 2017. https://doi.org/10.1016/j.ijadhadh.2017.02.003.
11. Galvez P, Noda NA, Takaki R, Sano Y, Miyazaki T, Abenojar J, Martínez MA. Intensity of singular stress field (ISSF) variation as a function of the Young's modulus in single lap adhesive joints. Int J Adhe Adhes. 2019. https://doi.org/10.1016/j.ijadhadh.2019.102418.
12. Liew K, Shahsavan H, Zhao B. Functionally graded dry adhesives based on film-terminated silicone foam. Int J Adhes Adhes. 2017. https://doi.org/10.1016/j.ijadhadh.2017.02.009.
13. Nakanouchi M, Sato C, Sekiguchi Y, Haraga K, Uno H. Development of application method for fabricating functionally graded adhesive joints by two-component acrylic adhesives with different elastic moduli. J Adhes. 2019. https://doi.org/10.1080/00218464.2019.1583562.
14. Carbas RJC, da Silva LFM, Critchlow GW. Adhesively bonded functionally graded joints by induction heating. Int J Adhes Adhes. 2014. https://doi.org/10.1016/j.ijadhadh.2013.09.045.
15. Sancaktar E, Kumar S. Selective use of rubber toughening to optimize lap-joint strength. J Adhes Sci Technol. 2000. https://doi.org/10.1163/156856100742195.
16. Stapleton SE, Waas AM, Arnold SM. Functionally graded adhesives for composite joints. Int J Adhes Adhes. 2012. https://doi.org/10.1016/j.ijadhadh.2011.11.010.
17. da Silva CI, Cunha MRO, Barbosa AQ, Carbas RJC, Marques EAS, da Silva LFM. Functionally graded adhesive joints using magnetic microparticles with a polyurethane adhesive. J Adv Join Process. 2021. https://doi.org/10.1016/j.jajp.2021.100048.
18. Abenojar J, Barbosa AQ, Ballesteros Y, del Real JC, da Silva LFM, Martínez MA. Effect of surface treatments on cork: surface energy, adhesion and acoustic insulation. Wood Sci Technol. 2014. https://doi.org/10.1007/s00226-013-0599-7.
19. Abenojar J, López de Armentia S, Barbosa AQ, Martínez MA, Velasco F, da Silva LFM, del Real JC. Coating cork particles with iron oxide: effect on magnetic properties. Wood Sci Technol. 2020. https://doi.org/10.1007/s00226-020-01191-4.
20. da Silva C, Barbosa AQ, Marques JB, Carbas RJC, Marques EAS, Abenojar J, da Silva LFM. Mechanical characterisation of graded single lap joints using magnetised cork microparticles. Advanced joining processes. Singapore: Springer; 2020. p. 3–12.
21. Bahlakeh G, Ghaffari M, Saeb MR, Ramezanzadeh B, Proft FD, Terryn H. A close-up of the effect of iron oxide type on the interfacial interaction between epoxy and carbon steel: combined molecular dynamics simulations and quantum mechanics. J Phys Chem C. 2016. https://doi.org/10.1021/acs.jpcc.6b03133.
22. Shabanian M, Moghanian H, Khaleghi M, Hajibeygi M, Khonakdar HA, Vahabi H. Chitosan and imide-functional Fe_3O_4 nanoparticles to prepare new xanthene-based poly(ether-imide) nanocomposites. RCS Adv. 2016. https://doi.org/10.1039/C6RA15744K.
23. Jouyandeh M, Reza-Paran MS, Shabanian M, Ghiyasi S, Vahabi H, Badawi M, Formela K, Puglia D, Reza M. Curing behavior of epoxy/Fe_3O_4 nanocomposites: a comparison between the effects of bare Fe_3O_4, Fe_3O_4/SiO_2/chitosan and Fe_3O_4/SiO_2/chitosan/imide/phenylalanine-modified nanofillers. Prog Org Coat. 2018. https://doi.org/10.1016/j.porgcoat.2018.06.006.
24. Jouyandeh M, Ali JA, Aghazadeh M, Formela K, Reza-Saeb M, Ranjbar Z, Reza-Ganjali M. Curing epoxy with electrochemically synthesized $ZnxFe_3$-xO_4 magnetic nanoparticles. Prog Org Coat. 2019. https://doi.org/10.1016/j.porgcoat.2019.105246.
25. Salehirad M, Nikje MMA, Alam LA. Synthesis and characterization of functionalized Fe_3O_4/Boron nitride as magnetically alignable 2D-nanofiller to improve the thermal conductivity of epoxy nanocomposites. Ind Eng Chem Res. 2018. https://doi.org/10.1021/acs.iecr.7b03540.
26. Li J, Zhang G, Zhang H, Fan X, Zhou L, Shang Z, Shi X. Electrical conductivity and electromagnetic interference shielding of epoxy nanocomposite foams containing functionalized multi-wall carbon nanotubes. Appl Surf Sci. 2018. https://doi.org/10.1016/j.apsusc.2017.08.234.
27. Zheng T, Wang X, Lu C, Zhang X, Ji Y, Bai C, Chen Y, Qiao Y. Studies on curing kinetics and tensile properties of silica-filled phenolic amine/epoxy resin nanocomposite. Polymers. 2019. https://doi.org/10.3390/polym11040680.
28. Abenojar J, Martínez MA, Pantoja M, Velasco F, del Real JC. Epoxy composite reinforced with nano and micro SiC particles: curing kinetics and mechanical properties. J Adhes. 2012. https://doi.org/10.1080/00218464.2012.660396.
29. Paz-Abuín S, López-Quintela A, Pazos-Pellín M, Paz-Pazos M. Influence of the reactivity of amine hydrogens and the evaporation of monomers on the cure kinetics of epoxy-amine: kinetic questions. Polymer. 1997. https://doi.org/10.1016/S0032-3861(96)00957-3.
30. Horie K, Hiura H, Sawada M, Mita I, Kambe H. Calorimetric investigation of polymerization reactions III. Curing reaction of

epoxides with amines. J Polym Sci A Polym Chem. 1970. https://doi.org/10.1002/pol.1970.150080605.
31. Erdogan B, Seyhan A, Ocak Y. Cure kinetics of epoxy resin-natural zeolite composites. J Therm Anal Calorim. 2008. https://doi.org/10.1007/s10973-008-9366-7.
32. Tikhani F, Moghari S, Jouyandeh M, Laoutid F, Vahabi H, Reza-Saeb M, Dubois P. Curing kinetics and thermal stability of epoxy composites containing newly obtained nano-scale aluminum hypophosphite (AlPO2). Polymers. 2020. https://doi.org/10.3390/polym12030644.
33. Barbosa AQ, da Silva LFM, Abenojar J, del Real JC, Paiva RMM, Öchsner A. Kinetic analysis and characterization of an epoxy/cork adhesive. Thermochim Acta. 2015. https://doi.org/10.1016/j.tca.2015.01.025.
34. Oliveira V, Pereira H. Cork and cork stoppers: quality and performance. London: IntechOpen; 2020.
35. Genevaus C, Bounoure GCORK. Architecture, design, fashion, and art. California: Gingko Press, Incorporated; 2020.
36. Jové-Martín P, Verdum-Virgos M. Cork science and its applications II. Pennsylvania: Materials Research Forum LLC; 2019.
37. Kissinger HE. Reaction kinetics in differential thermal analysis. Anal Chem. 1957. https://doi.org/10.1021/ac60131a045.
38. Vyazovkin S, Wight CA. Model-free and model-fitting approaches to kinetic analysis of isothermal and non-isothermal data. Thermochim Acta. 1999. https://doi.org/10.1016/S0040-6031(99)00253-1.
39. Sewry JD, Brown ME. "Model-free" kinetic analysis? Thermochim Acta. 2002. https://doi.org/10.1016/S0040-6031(02)00083-7.
40. Hakvoort G, van Reijen L. Measurement of the thermal conductivity of solid substances by DSC. Thermochim Acta. 1985. https://doi.org/10.1016/0040-6031(85)85081-4.
41. Boddington T, Laye PG. The measurement of thermal conductivity by differential scanning calorimetry. Thermochim Acta. 1987. https://doi.org/10.1016/0040-6031(87)88380-6.
42. Yates F. The design and analysis of factorial in experiments. Imperial bureau of soil science. Harpenden: Hafner Press (Macmillan); 1937.
43. Heiberger RM. Yates' algorithm for factorial designs in computation for the analysis of designed experiments. New York: Wiley; 2015. p. 258–93.
44. Martínez MA, López de Armentia S, Abenojar J. Influence of sample dimensions on single lap joints: effect of interactions between parameters. J Adhes. 2021. https://doi.org/10.1080/00218464.2020.1771313.
45. Socrates G. Infrared and Raman characteristics group frequencies. 3rd ed. West Sussex: Wiley; 2001.
46. Huo R, Zhang Z, Athir N, Fan Y, Liu J, Shi L. Designing high thermal conductivity of cross-linked epoxy resin via molecular dynamics simulations. Phys Chem Chem Phys. 2020. https://doi.org/10.1039/D0CP02819C.
47. Mojun L, Peiyi W, Yifu D, Shanjun L. Study on diffusion behavior of water in epoxy resins cured by active ester. Phys Chem Chem Phys. 2003. https://doi.org/10.1039/B208782K.